Modelling natural images with multifractal multiplicative cascades

Ibrahim Ayed

February 26, 2018

Abstract

In this work, we present a multifractal model for images from the work of Pierre Chainais, starting from two of his papers, [3] and [4]. We begin by motivating the approach and showing the logical steps leading to the construction of this model then we outline its usefulness to synthesize complex turbulent textures and demonstrate an application in virtual super-resolution.

Introduction

Studying the Fourier spectrum of turbulent natural images or moments of their statistics clearly shows that those images have a scale invariant structure, at least on some range of scales. The complexity of such a structure which have been extensively studied over the last few decades justifies the use of stochastic processes with the same scale invariance in order to model those images and better understand their underlying structure. Empirical evidence shows that this structure is not limited to its second order statistics and thus is not gaussian as many works generally suppose. The processes we present in this work are stochastic non-gaussian scale-invariant processes and should thus be flexible enough to cover a wide variety of complex images.

We will be more particularly interested here in the special case of *Compound Poisson Cascades*. One advantage of CPCs is that they can be easily generated and thus are natural candidates for synthesizing realistic turbulent textures. This will be our first application of the studied model. We will see that the possibilities are very rich and that there are many variations using CPCs. Moreover, as opposed to models such as the one in [5] which may suffer from blocking effects when doing local operations on the generated images, such modifications are very easy in CPCs, especially "zooming in".

Actually, one of the greatest advantages of CPCs is that they make changes in the finer scales very natural conceptually and easy computationally. This corresponds to the usual idea of images not having any natural notion of characteristic length or scale : The finest scale only depends on the resolution of the image and thus can vary, even for the same object, pictured from the same point of view, with the same lighting,... A straightforward idea of application to this observation is then to add, given a turbulent image, information at the sub-pixel level, thus enhancing the resolution of the image in a way that is coherent with its structure. There are several methods used as an answer to this problem, from B-Spline interpolation and other advanced interpolation methods which just does a more or less sophisticated smoothing of the image at lower resolutions to methods focusing on edges which works on simply structured images but not on turbulent ones to methods which actually try to make use of local scale invariance, often through a wavelet analysis of the image such as in which is actually quite similar to the approach we present in spirit but is deterministic and too sensitive to arbitrary choices.

1 Modelling images with scale invariant processes

In this first part, we introduce the models we will be using then derive some useful properties.

1.1 Self-similarity, Multifractal processes and Infinitely Divisible Cascades

1.1.1 Self-similar processes

The most intuitive idea to mathematically formalize the fact that a certain 1D process X has a similar aspect when visualized at different scales is to state that $X(ct)$ and $X(t)$ should be equal in some sense for every positive c, maybe with some restrictions over c if such invariance is not true for any considered scale. This can be written as :

$$\{X(ct)\} \stackrel{d}{=} c^H \{X(t)\}$$

where H is the Hurst parameter of X and this equality means that $(X(ct_1), ..., X(ct_k))$ and $(c^H X(t_1), ..., c^H X(t_k))$ have the same distribution. Such stochastic processes are coined in the literature as *self-similar* ones. This definition can be relaxed into that of *multiscaling processes* by restricting the range of t to a certain scale T and replacing c^H by $W_c = c^H e^{\Omega_c}$ where Ω_c is an independent real random variable such that[1] $\mathbb{E}(e^{q\Omega_c}) = c^{\tau(q)}$ with τ a concave function.

1.1.2 Multifractal processes

For modelling, only processes with some stationarity can be of interest. Thus, following the definitions above, one can consider a process X with multiscaling and stationary increments so that we have, whenever those quantities exist, for $\delta_r X(t) = X(t+r) - X(t)$ and keeping the same notations :

$$\forall r \in [0, T],\ \mathbb{E}|\delta_r X|^q = \mathbb{E}|\delta_1 X|^q\ r^{qH+\tau(q)}$$

Relaxing this definition for small increments r and generalizing to higher dimensions yields the following definition :

Definition 1 (Multifractal processes)**.** A stochastic process X in $\mathbb{R}^d$ is *multifractal* when :

$$\forall q_- \leq q \leq q_+,\ \mathbb{E}|T_r(X)|^q \stackrel{r\to 0}{\sim} C_q r^{\zeta(q)}$$

with $\zeta(q) = qH + \tau(q)$ the *multifractal exponents*, τ concave and $T_r(X)$ is a *multiscale statistic* of X at scale r.

In the case of images, which we will focus on for the remaining of this work, the multiscale statistics can be for example box averages of the intensity, wavelet coefficients,...

To be more rigorous, multifractality should actually defined through the local *Hölder exponents* of the process which express its local regularity and the so-called *Multifractal formalism* defines the conditions under which those can be characterized by more global (and computable !) quantities as in definitions such as the one above, which approach can be seen, for example, in [6]. But it is out of the scope of this work to delve further in those details.

1.1.3 From multiscaling to Infinitely Dvisible Cascades

However, the last definition is still too restrictive for modelling purposes as it only focuses on the finer scales while one usually observes scale invariance over a range of scales $[r_{\min}, r_{\max}]$. Thus, we define instead the multiscaling property by :

$$\forall q_- \leq q \leq q_+,\ \forall r_{\min} \leq r \leq r_{\max},\ \mathbb{E}|T_r(X)|^q\ =\ C_q r^{\zeta(q)}$$

Following the reasoning in chapter 2 of [1], we can write, for $r_1, r_2 \in [r_{\min}, r_{\max}]$:

$$\mathbb{E}[e^{q \log |T_{r_2}(X)|}] = \exp\{-\zeta(q)[-\log r_2 - (-\log r_1)]\}\mathbb{E}[e^{q \log |T_{r_1}(X)|}]$$

[1] This relation has to be true at least for q in some relevant range.

By defining $n(r) = -\log r$ and G a random variable such that its moment generating function is $\tilde{G}(q) = e^{-\zeta(q)}$, we have that :

$$\mathbb{E}[e^{q \log |T_{r_2}(X)|}] = \tilde{G}(q)^{n(r_2)-n(r_1)} \mathbb{E}[e^{q \log |T_{r_1}(X)|}]$$

then going back to probabilities gives :

$$\mathbb{P}_{\log |T_{r_2}(X)|} = \mathbb{P}_G{}^{\star[n(r_2)-n(r_1)]} \star \mathbb{P}_{\log |T_{r_1}(X)|}$$

For this last expression to have a meaning, when $n(r_2) - n(r_1)$ is not an integer, for the convolution power of $\mathbb{P}_G$ to be defined, G needs to be infinitely divisible in the sense that, for every integer n, there are $X_1, ..., X_n$ *i.i.d.* such that they sum to a variable with the same distribution as G.

Then, going back to $T_r(X)$, we see that it has an inherent multiplicative structure as we can write :

$$|T_{r_2}(X)| = W |T_{r_1}(X)|$$

where $W = e^w$, w being distributed as $\mathbb{P}_G{}^{\star[n(r_2)-n(r_1)]}$, is log-infinitely divisible and only depends on[2] $n(r_2) - n(r_1)$.

Conversely, we can easily see, by going back through the previous derivation, that a process X such that $T_r(X)$ obeys a log-infinitely divisible multiplicative cascade verifies, for any q and any r_2, r_1 in the range of scales of the cascade :

$$\frac{\mathbb{E}|T_{r_2}(X)|^q}{\exp\{-\zeta(q) n(r_2)\}} = \frac{\mathbb{E}|T_{r_1}(X)|^q}{\exp\{-\zeta(q) n(r_1)\}}$$

which takes us back to the multiscaling power law when $n(r) = -\log r$.

1.2 Compound Poisson Cascades

Having thus shown in the previous section the profound links between scale invariance and multiplicative cascades, it comes now naturally that multiscaling processes can be defined through multiplicative cascades. Keeping the previous notations, if we choose a distribution for W, or equivalently for G, a construction for such a process stems naturally from the multiplicative cascade. The only restrictions arise when if we want it to follow the multifractal power law and if we want to control the multifractal exponents of the process, for example if we want it to fit the statistical properties of some available signal.

In this section, we construct the so-called *Compound Poisson Cascades* which are a family of IDCs having the advantage of being easy to synthesize. First of all, let us define :

Definition 2 (Cone of influence)**.** The *cone of influence* is the set of $\mathbb{R}^d \times \mathbb{R}^+$, defined for every $x \in \mathbb{R}^d$ as :

$$\mathcal{C}_l(x) = \left\{ (x', r') \ : \ l \leq r' \leq 1, \ \|x' - x\| < \frac{r'}{2} \right\}$$

The intuition behind CPC is that each point of the process should be the result of the multiplication of random factors coming from the different scales defined by the cone[3]. This can be done by defining a Poisson point process (x_i, r_i) with density $dm(x, r) = dx \frac{1}{r^{d+1}} dr$, a choice which ensures shift invariance and power law scaling[4], as well as associated *i.i.d.* positive multipliers (W_i) so that we can define :

Definition 3 (Compound Poisson Cascade)**.** With the same notations, a *Compound Poisson Cascade* is defined by :

$$\mathcal{Q}_l(x) = \frac{1}{C} \prod_{(x_i, r_i) \in \mathcal{C}_l(x)} W_i$$

where C is a normalization constant. The relevant range of scales for this process is naturally defined through $\mathcal{C}_l$ namely $[l, 1]$. Changing the scaling range then amounts to a change of variables by defining :

$$Q_l^L(x) = Q_l\Big(\frac{x}{L}\Big)$$

[2]Here $n(r_2) - n(r_1) = \log \frac{r_1}{r_2}$ but n could be generalized to any other non increasing function of r. This form allows however to keep the power law scaling corresponding to multifractals.

[3]This can be seen as a generalization of classical constructions such as Mandelbrot's binomial cascade. However, this construction has the advantage of being shift-invariant and thus stationary.

[4]See the Appendix A of [2] for a derivation of this expression.

Taking the logarithm in the previous definition, we get :

$$\log \mathcal{Q}_l(x) = \sum_{(x_i,r_i)\in\mathcal{C}_l(x)} \log W_i - \log C$$

which can also be written as, denoting by $\mathcal{D}(a,b)$ the disk of center a and radius b :

$$\log \mathcal{Q}_l(x) = \sum_i \mathbb{1}_{\mathcal{D}(x_i,r_i/2)}(x) \log W_i - \log C$$

so that we can replace the indicating function by another function f which gives the generalization :

$$\log \mathcal{Q}_l(x) = \sum_i f\Big(\frac{x-x_i}{r_i}\Big) \log W_i - \log C'$$

This last form has the advantage of being richer and thus will be useful when synthesizing textures for example as we will in the next part. However, with more complexity comes the difficulty of controlling features of the generated CPC including its multifractal exponents, which is important when fitting the CPC to a given signal, whereas the first form has its exponents directly controlled through the moments of the W_i through the formula[5] :

$$\tau(q) = q(\mathbb{E}W_i - 1) + 1 - \mathbb{E}W_i^q$$

Let us also note that, for CPCs, we have $H = 0$.

Finally, it is also possible to calculate the normalization constant C for Q_l as :

$$C = \mathbb{E}\Big[\prod_{(x_i,r_i)\in\mathcal{C}_l(x)} W_i\Big] = r^{\mathbb{E}W-1}$$

[5]See 3.2. of [2] for a quick derivation of this formula.

2 Numerical analysis and experiments

This part uses the formalism defined in the previous to synthesize and zoom into complex textured 2D images.

2.1 Generating textures

Let us now present the steps of the algorithm[6] we used to generate a 2D CPC Q_l on the domain $[X_{\min}, X_{\max}] \times [Y_{\min}, Y_{\max}]$:

1. Generate the number of points N following a Poisson process of parameter $\lambda = \frac{2}{\pi} \times (X_{\max} - X_{\min}) \times (Y_{\max} - Y_{\min}) \times (\frac{1}{l^2} - 1)$.
2. Sample N points (x_i, y_i, r_i) where the x_i are uniformly chosen on $[X_{\min}, X_{\max}]$, the y_i are uniformly chosen on $[Y_{\min}, Y_{\max}]$ and the r_i have a density proportional to $\frac{1}{r^2}$ on $[l, 1]$.
3. Sample the corresponding $\log W_i$ from a chosen distribution.
4. Construct a grid for the target domain and, for each point of the grid x, sum the $f(\frac{x-x_i}{r_i}, \frac{y-y_i}{r_i}) \log W_i$ for i such that $(x_i, y_i) \in \mathcal{C}_l(x)$, take the exponential and normalize the result : this is $Q_l(x)$.

As we have seen previously, a CPC has $H = 0$ in its multifractal exponents. In order to have even more possibilities we can also fractionally integrate the result of the algorithm in order to have $H > 0$.

We can see from this algorithm that there are many ways to alter its outcome, here is a sample from what we have studied here :

The distribution of $\log W_i$ Here we have considered a normal distribution $\log W_i^{(1)}$ with parameters μ and σ as well as a distribution $\log W_i^{(2)}$ such that $W = (1+T)u^T$ where T is a parameter and u is uniformly sampled from $[0, 1]$. Figures 5 and 1 show examples of the differences between textures generated with those two distributions.

The function f We have considered here the following functions :

- the constant 1, which just corresponds to taking multipliers in $C_l(x)$;
- $f_2(x, y) = \mathbb{1}_{\|(x,y)\|_1 \leq 0.5}$;
- $f_3(x, y) = \mathbb{1}_{\|(x,y)\|_2 \leq 0.5} \cos\left(\pi \left\|(\frac{x}{a}, \frac{y}{b})\right\|_2\right)$;
- $f_4(x, y) = \mathbb{1}_{\|(x,y)\|_2 \leq 0.5} \cos\left(\pi \left\|(\frac{x}{a}, \frac{y}{b})\right\|_2\right)^2$;
- $f_5(x, y) = \mathbb{1}_{\|(x,y)\|_2 \leq 0.5} \cos\left(\pi e^{\left\|(\frac{x}{a}, \frac{y}{b})\right\|_2}\right)^2$;
- $f_6(x, y) = \mathbb{1}_{\|(x,y)\|_2 \leq 0.5} \cos\left(\pi e^{e^{\left\|(\frac{x}{a}, \frac{y}{b})\right\|_2}}\right)^2$;
- $f_7(x, y) = \mathbb{1}_{\|(x,y)\|_2 \leq 0.5} \exp\left\{-\frac{1}{1-(2\left\|(\frac{x}{a}, \frac{y}{b})\right\|_2)^4}\right\}$;

Figures 2 and 3 shows examples of textures generated by those different functions.

The anisotropy in f Playing on the values of a and b can alter the isotropy of the textures. Figure 4 shows examples of this.

The integration parameter H Figure 1 shows an example of the influence of H.

Our goal here was to show the richness of the set of textures the CPCs can generate. This can easily be extended to generating textures on manifolds, in higher dimensions,...

[6] Which is adapted from [2].

2.2 Multifractal virtual super-resolution

2.2.1 Formulation of the problem and algorithm

Starting from the hypothesis that the multifractal formalism we developped earlier are expressive enough to be good models for complex natural images : To be more precise, judging by the images we were able to synthesize in the previous section, those models should be good for textured images with scale invariance over some range of scales. A natural idea is then to use this model to interpolate this kind of images and solve the super-resolution problem : Given an image at a certain resolution, try to construct an image with a better resolution that is coherent with the initial one. As there is no ground truth to compare to in this formulation, the properties of a desirable solution have to be defined in an indirect way. Following the methodology of [4], we define two constraints on potential high resolution candidates :

Statistical consistency Extending the scale invariance to the higher resolution generated image in a way that is coherent with the observed properties of the initial one ;

Physical consistency Conserving the energy of each pixel of the initial image in the generated one meaning that the intensities of the newly generated subpixels should sum to the intensity of the pixel from the initial image that those new pixels replace.

The answer to the first constraint stems naturally from the following property of CPCs, which is a consequence of its multiplicative construction :

$$Q_{r_2}^{r_0} \stackrel{d}{=} Q_{r_1}^{r_0}\, Q_{r_2}^{r_1}$$

where $Q_{r_2}^{r_1}$ is independent from $Q_{r_1}^{r_0}$. Thus, having a model where the fine scales are described with a CPC $Q_{r_1}^{r_0}$, one can easily extend it to finer scales. The second constraint is also easily satisfied as it is enough to normalize the result obtained through the algorithm in a final step where one ensures that the intensities of the pixels sum as they shoould.

Those considerations bring us to an algorithm which unfolds in the following steps, given an image I :

1. Determine the multifractal properties of I by calculating its corresponding coefficients $\tau(q)$ and H . This allows to write it as :

   $$I = I_0 + \alpha \mathcal{I}_H\{Q_{r_1}^{r_0} - \mathcal{A}(Q_{r_1}^{r_0})\}$$

   where $\mathcal{I}_H$ is a fractional integration operator, which allows to fit the CPC to the right value of H, I_0 is the mean of I and $\mathcal{A}(Q_{r_1}^{r_0})$ is the spatial average over the image of the realization of the process $Q_{r_1}^{r_0}$.

2. Interpolate I to the new resolution, with a spline interpolation for example, to have I_{interp}.

3. Calculate J_1, the fractional derivative of order H of I_{interp} which makes it correspond to $\alpha(Q_{r_1}^{r_0} - \mathcal{A}(Q))$.

4. Generate $Q_{r_2}^{r_1}$ independently, where r_2 corresponds to the new resolution, and replace $Q_{r_1}^{r_0}$ by $Q_{r_1}^{r_0}\, Q_{r_2}^{r_1}$ in J_1 which gives :

   $$J_2 = J_1\, Q_{r_2}^{r_1} + \alpha \mathcal{A}(Q_{r_1}^{r_0})(Q_{r_2}^{r_1} - \mathcal{A}(Q_{r_2}^{r_1}))$$

5. Integrate J_2 into $K = I_0 + \mathcal{I}_H(J_2)$. Put the negative values[7] in K to 0.

6. Normalize K into I_2 to ensure conservation of energy as described above.

Even though this procedure seems to be straightforward, there are several catches to it. First of all, the first step supposes a thorough multifractal analysis of the class of the image I. The numerical stability of such an analysis is not trivial and won't be developed here but [8] presents a robust method for such an analysis based on a wavelet analysis of the signal[8].

[7] K is a matrix of light intensities so it should be positive and the integration operation could make it negative.

[8] A toolbox is even available on the website of one of the authors, Herwig Wendt.

A second set of unknown quantities arise in step 4 where one needs to have α and $\mathcal{A}(Q_{r_1}^{r_0})$ in order to calculate J_2. For $\mathcal{A}(Q_{r_1}^{r_0})$, as it is an empirical average of a process with mean 1, we just suppose it to be equal to 1. As for α, we can write the variance of J_1 and, using the power law scaling of order 2 for Q, we deduce the estimate :

$$\widehat{\alpha} = \sqrt{\frac{\widehat{var(J_1)}}{(\frac{r_1}{r_0})^{\tau(2)} - 1}}$$

This in turn needs the value of r_0 which is not straightforward to obtain but, as is shown in [4], the solution is not very sensitive with respect to the chosen value.

Another important feature of this procedure is that steps do not commutate and thus doing several successive magnifications $k_1, ..., k_n$ or a single one $k_1 \times \cdots \times k_n$ won't give the same result. We will follow in this work the author of [4] in preferring the first approach.

2.2.2 Results

Now that we have defined our approach, we can test it on concrete examples.

We start, with a synthesized one : We chose a mean I_0, an order H, α and generate a CPC Q to form a model as in step 1 of the algorithm. Thus, here we know all the parameters of the model so there is nothing to estimate. A sample of obtained results is shown in figure 6 where we go from a 32×32 to a 256×256 image. Figure 7 shows a detail of the image so that the effect of the super-resolution procedure is more noticeable. From a visual point of view, the results seem to be satisfying.

As in the studied paper [4], we apply the algorithm to an image from the Quiet Sun dataset[9] that can be seen in figure 8. Figure 9 shows the results. We have used here the distribution $\log W_i^{(2)}$ with the same parameters as in [7] which come from a multifractal analysis of the dataset : $T = 0.85$ and $H = 0.55$. One could certainly improve on those results by doing a more precise analysis of the image we zooming on here.

[9] The image was retrieved with a Google Images search so it might not be of the same quality as the one in the paper. There is actually no guarantee that we are using the same picture at all.

Conclusion

We have presented in this work a model for natural images which allows ta take into account structure related to scale invariance properties. We have thus presented the multifractal approach, how it leads naturally to Infinitely Divisible Cascades and more particularly focused on a family of IDC processes : Compounds Poisson Cascades. Those easy to generate and highly parameterizable processes allow to synthesize a wide variety of turbulent textures which can be adapted to many settings. We have also studied an approach using the properties of those processes to build a virtual super-resolution algorithm. This approach is non-deterministic, thus potentially generating an infinity of high resolution candidates for the same image and is more importantly physically and statistically coherent with the initial image.

However, let us stress the fact that what we presented in this work only works well for turbulent and textured natural images and for a limited range of scales : Zooming out too much from an image or trying it on cartoon images wouldn't correspond to the model. Furthermore, a mixture of different textures in separate zones of the image would need to be treated separately. Moreover, one important catch in the two applications we presented here is the need to know the multifractal structure of the image, which can be done as there are now toolboxes which can do it, but also to be able to find the right parameters to reproduce. For example, in the example of the Quiet Sun image, the author has handcrafted a distribution for the W_is to make a model suited to the observed multifractal exponents.

Thus, in order to be able to generate textures online or to zoom into a previously unknown texture, there is a need to build method for estimating the corresponding parameters of the CPC. This could be an interesting direction of work to make use of this model.

References

[1] Pierre Chainais. *Cascades log-infiniment divisibles et analyse multiresolution. Application a l'etude des intermittences en turbulence.* PhD thesis, ENS Lyon, 2001.

[2] Pierre Chainais. Multidimensional infinitely divisible cascades. application to the modelling of intermittency in turbulence. *The European Physics Journal B*, 2006.

[3] Pierre Chainais. Infinitely divisible cascades to model the statistics of natural images. *IEEE Transactions on pattern analysis and machine learning*, 2007.

[4] Pierre Chainais. Virtual super resolution of scale invariant textured images using multifractal processes. *Journal of Mathematical Imaging and Vision*, 2011.

[5] Eero P. Simoncelli Martin J.Wainwright and Alan S. Willsky. Random cascades on wavelet trees and their use in analyzing and modeling natural images. 2000.

[6] R.H. Riedi. Multifractal processes. 2003.

[7] P. Chainais V. Delouille and J.-F. Hochedez. Quantifying and containing the curse of high resolution coronal imaging. *Annales Geophysicae*, 2008.

[8] Herwig Wendt, Stephane G. Roux, Patrice Abry, and Stephane Jaffard. Wavelet leaders and bootstrap for multifractal analysis of images. *Signal Proces.*, 89:1100–1114, 2009.

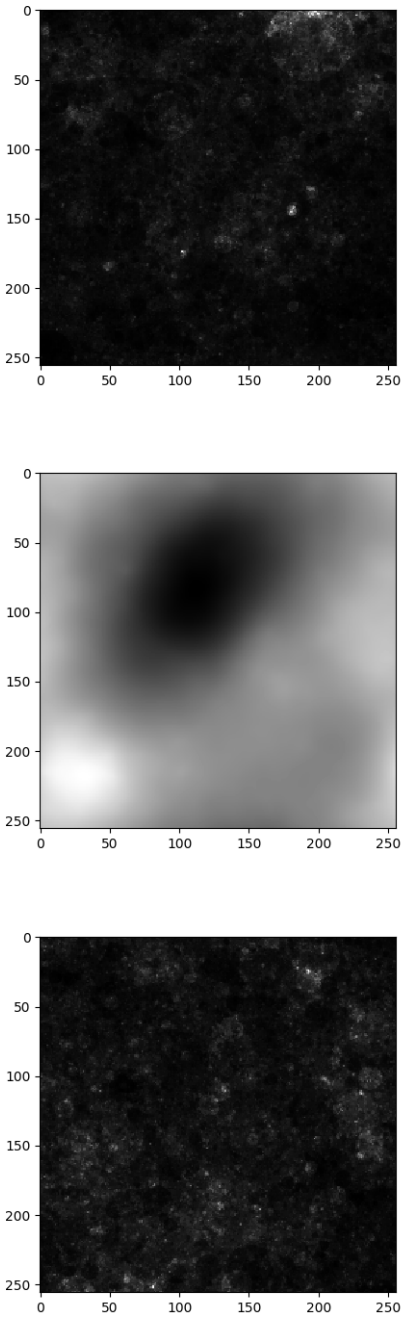

Figure 1: Integrated constant function CPCs of log-normal distribution with parameters, from top to down : $H = 0.05$, $\mu = -0.04$ and $\sigma = \sqrt{0.08}$; $H = 1$, $\mu = -0.04$ and $\sigma = \sqrt{0.08}$; $H = 0.05$, $\mu = -0.004$ and $\sigma = \sqrt{0.08}$.

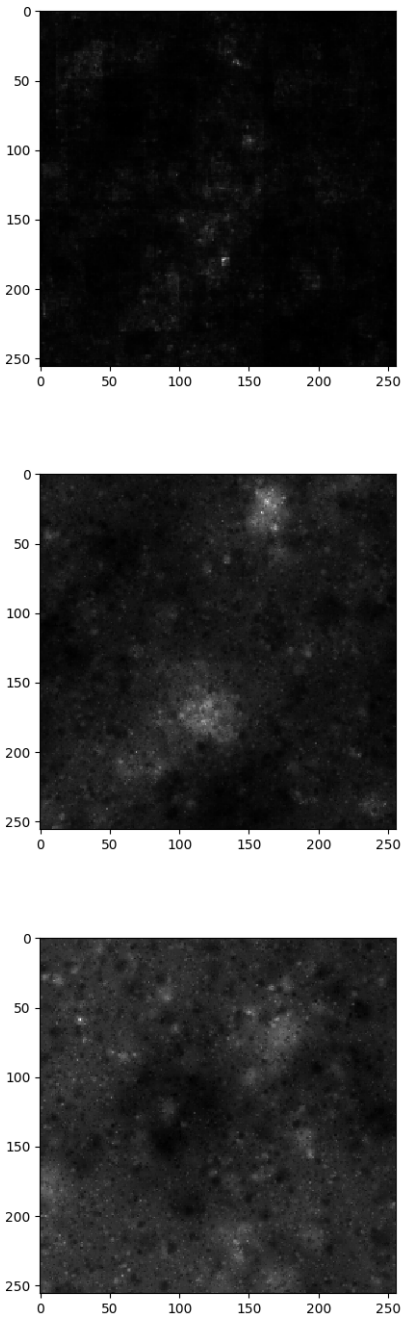

Figure 2: Integrated CPCs of log-normal distribution ($\mu = -0.04$ and $\sigma = \sqrt{0.08}$) with $H = 0.05$ with functions, from top to down : f_2, f_3, f_4. For all functions where this is relevant we have taken an isotropic setting with $a = b = 1$.

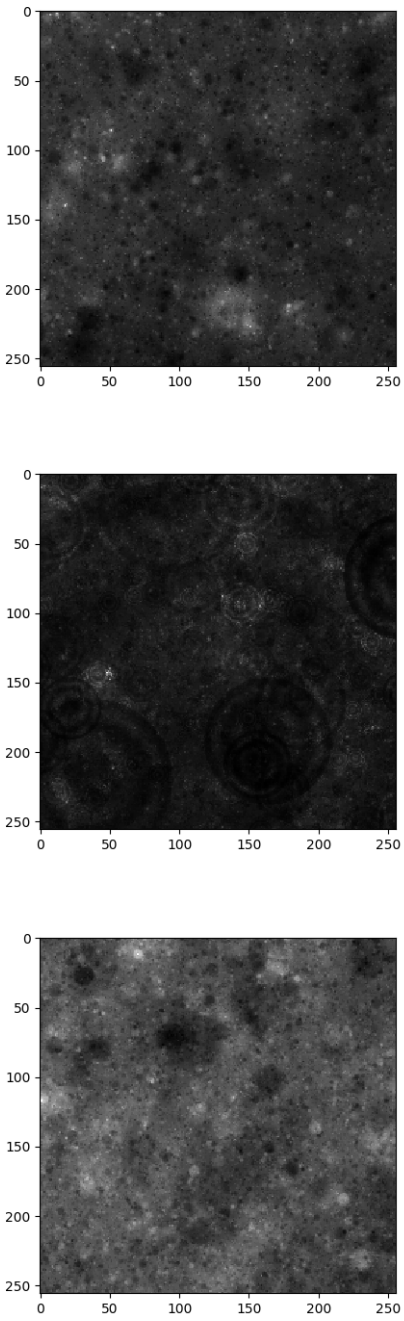

Figure 3: Integrated CPCs of log-normal distribution ($\mu = -0.04$ and $\sigma = \sqrt{0.08}$) with $H = 0.05$ with functions, from top to down : f_5, f_6, f_7. For all functions where this is relevant we have taken an isotropic setting with $a = b = 1$.

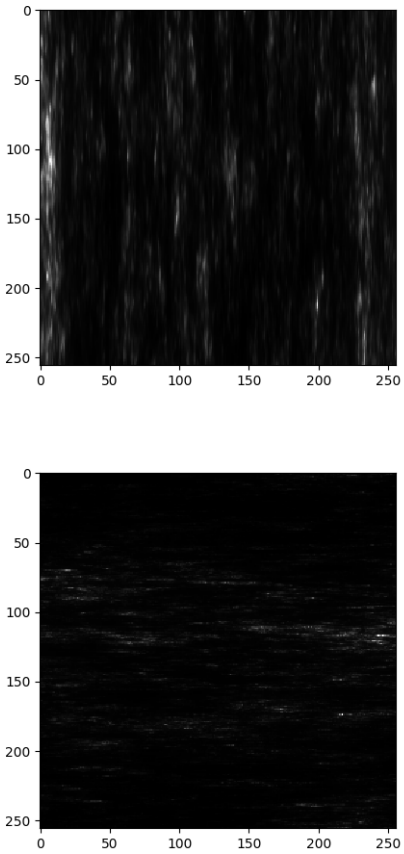

Figure 4: Integrated CPCs of log-normal distribution ($\mu = -0.04$ and $\sigma = \sqrt{0.08}$) with $H = 0.05$ with functions, from top to down : f_3 with $a = 1$ and $b = 10$; f_6 with $a = 10$ and $b = 1$.

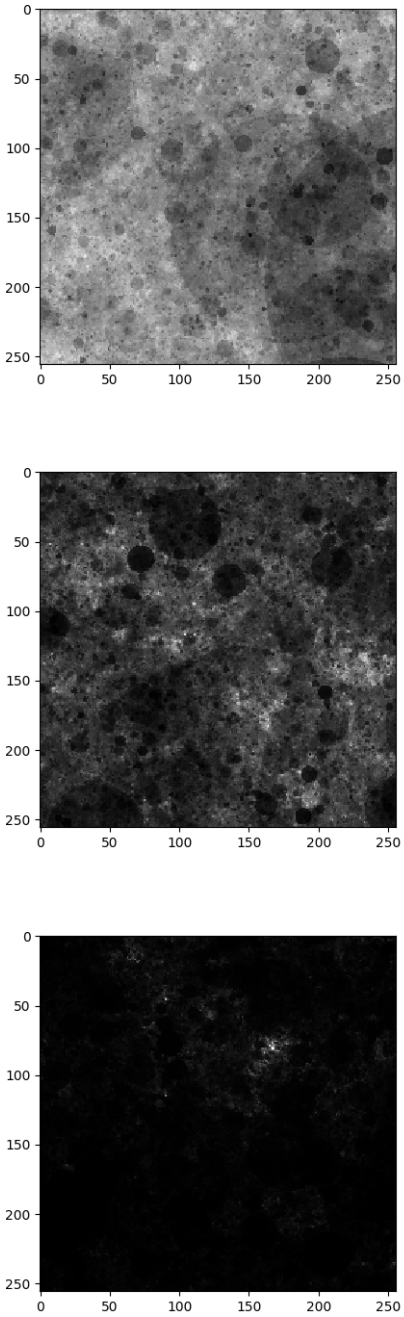

Figure 5: Integrated CPCs of distribution $\log W^{(2)}$ with $H = 0.05$ and, from top to down : $T = 0.08$, $T = 0.3$, $T = 0.8$.

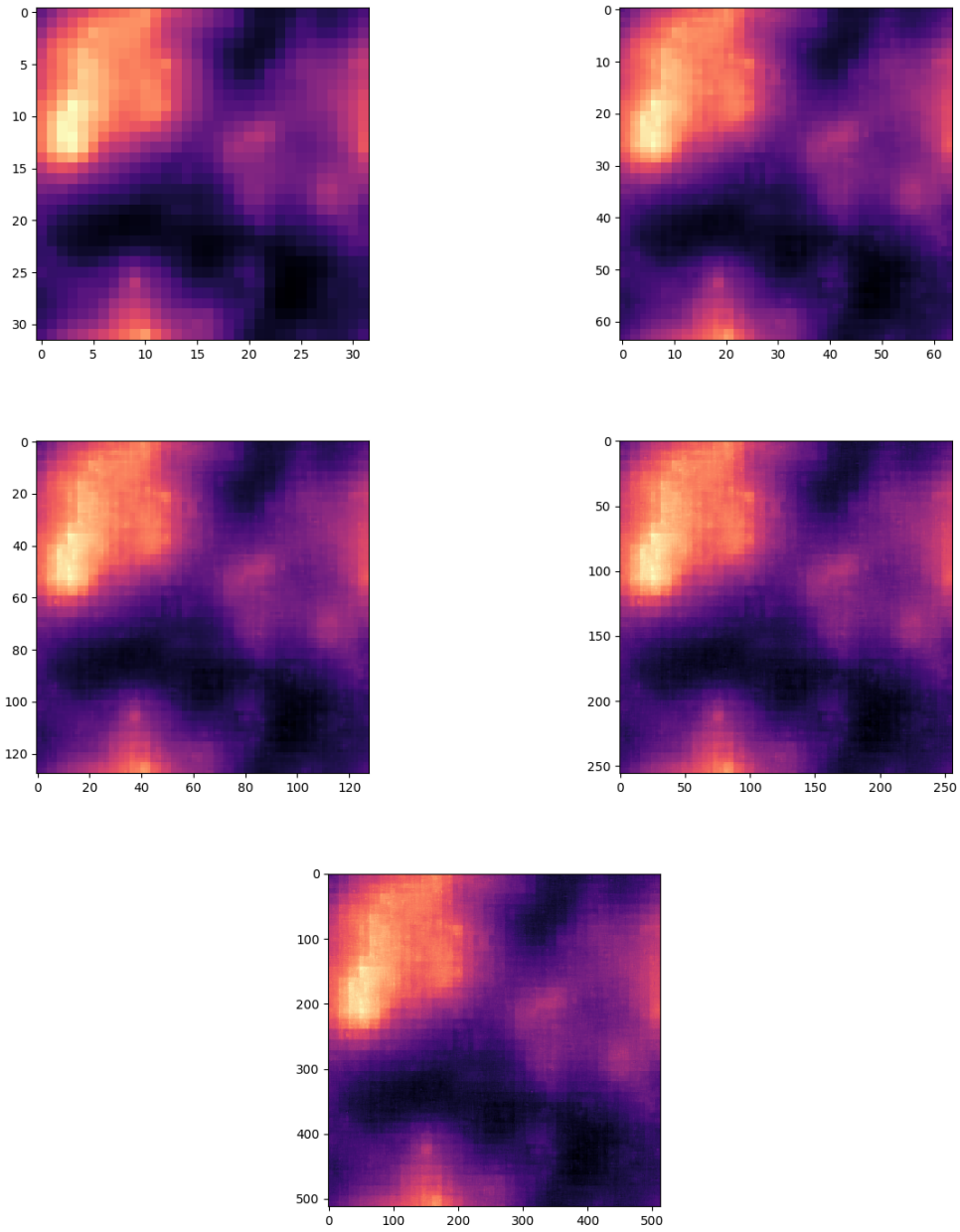

Figure 6: From top to down, left to right : a 32×32 integrated CPC as in step 1 of the algorithm with $alpha = 8$, $H = 0.7$, $I0 = 23$; its $\times 2$ magnification using the super-resolution algorithm ; its $\times 4$ magnification ; its $\times 8$ magnification ; its $\times 16$ magnification.

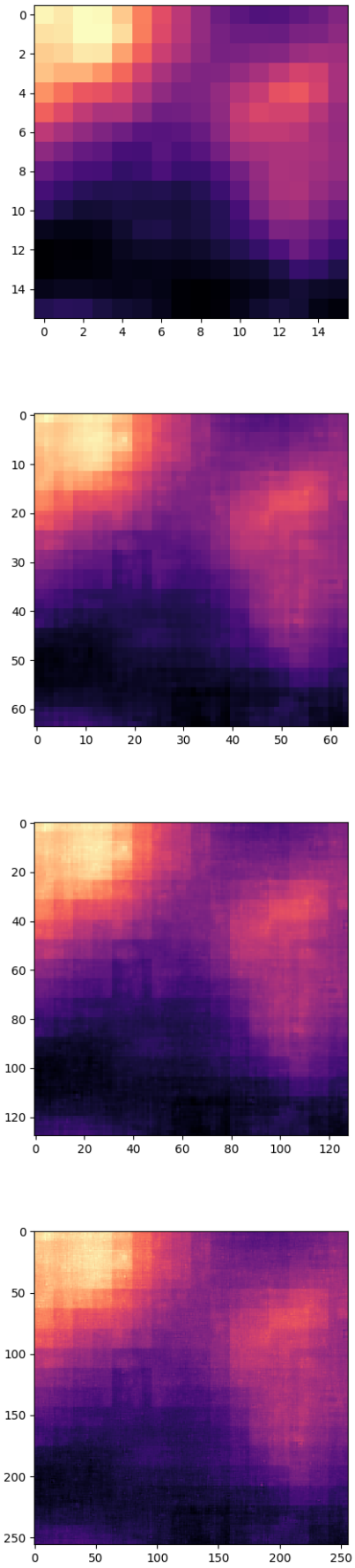

Figure 7: From top to down : a 16×16 detail of the CPC from figure 6 ; its $\times 4$ magnification ; its $\times 8$ magnification ; its $\times 16$ magnification.

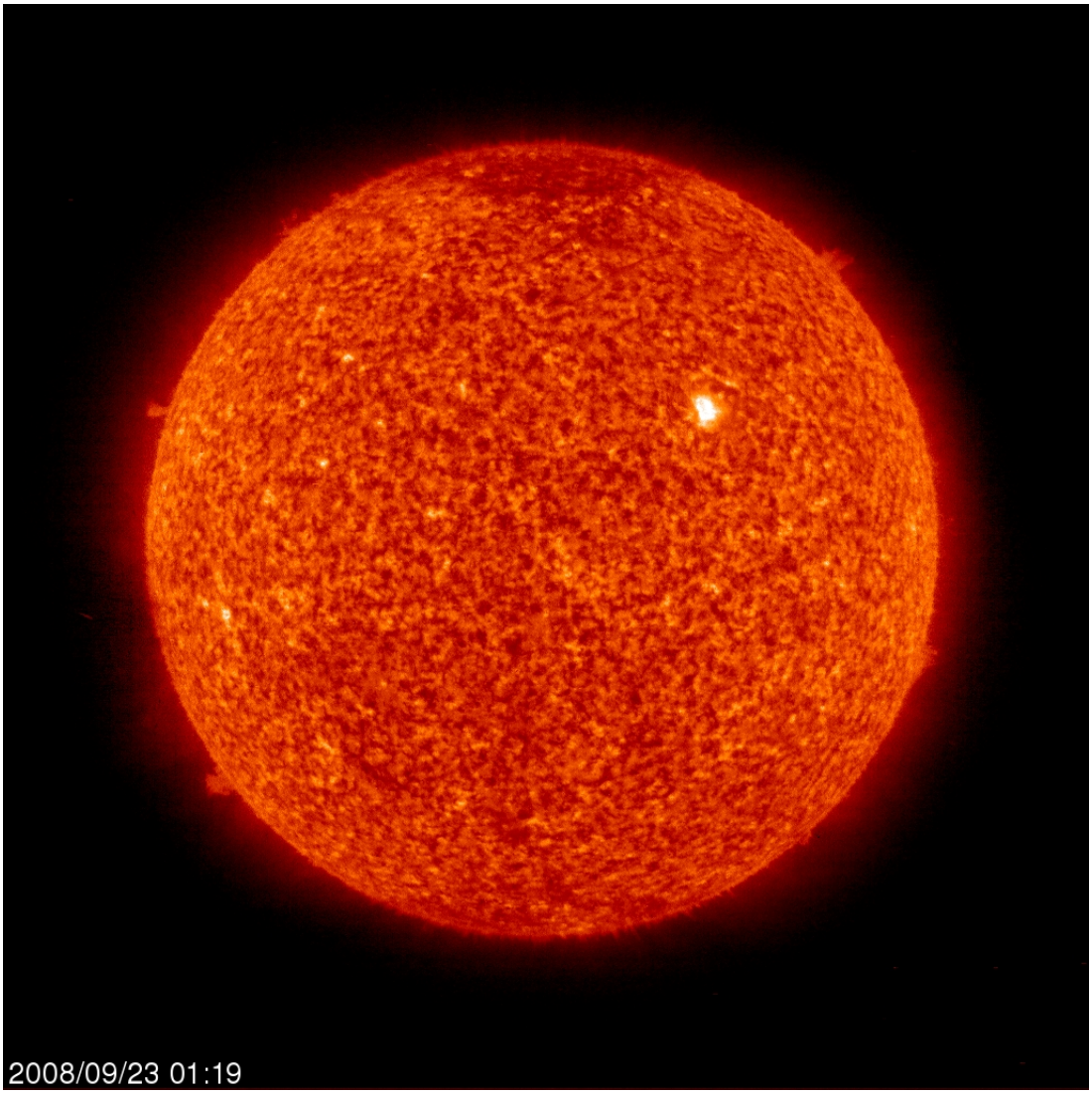

Figure 8: Photo taken from the Quiet Sun dataset

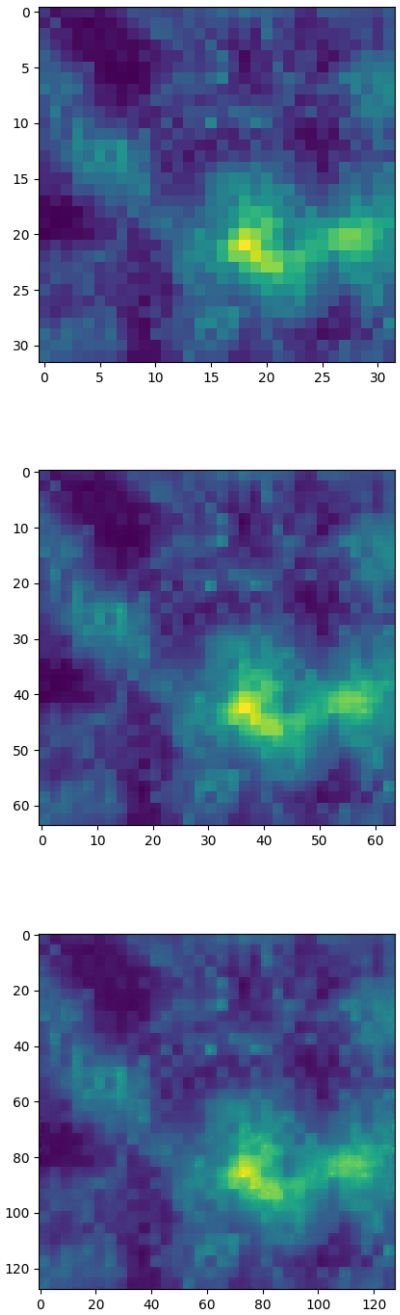

Figure 9: From top to down : A 32×32 detail from the photo in figure 8, the detail magnified $\times 2$, $\times 4$ of the detail. The super-resolution algorithm is executed with $\log W^{(2)}$, $T = 0.85$, $H = 0.55$.